

文章编号:0253-4339(XXXX)XX-0001-17

doi: 10.12465/issn.0253-4339.20260318003

## 柔性热电器件研究进展

晏君豪<sup>1</sup> 申利梅<sup>1</sup> 刘志春<sup>1</sup> 叶冬<sup>2</sup>

(1 华中科技大学能源与动力工程学院 武汉 430074; 2 华中科技大学智能制造装备与技术全国重点实验室 武汉 430074)

**摘要** 柔性热电器件具备优良的弯曲能力与表面贴合特性,能够直接将非平面热源的低品位热能转化为电能或实现曲面的快速制冷,在可穿戴电子设备、物联网无线传感器的自供电及柔性电子器件冷却等领域展现独特优势,受到学术界与工业界的广泛关注。近十年柔性热电器件得到快速发展,尤其在开发高性能的柔性有机热电器件,发展薄膜化的柔性无机热电器件,构筑柔性基底与刚性材料结合的柔性热电器件等方面取得突破,目前柔性热电器件贴附于人体皮肤可输出1.6 mW的电能或产生约10 °C的冷却温差。随着柔性电子技术的持续演进,对自供电与冷却技术的需求日益提升,鉴于此,本文以柔性拓扑方案为主线,对柔性热电器件展开综述,通过定义热电臂的无量纲特征长度作为区分依据,将器件划分为一维纤维、二维膜状、三维块体3类。总结了该技术工程化应用面临的瓶颈问题,如受限环境下功率密度不足、低热阻封装技术缺失等,并展望了从结构设计到系统化集成层面的优化途径,旨在为柔性热电器件的实用化发展提供方向。

**关键词** 柔性热电器件;可穿戴器件;柔性拓扑方案;发电性能;制冷性能

中图分类号: TB61<sup>9</sup>.2;TB34

文献标识码: A

## Research Progress in Flexible Thermoelectric Devices

Yan Junhao<sup>1</sup> Shen Limei<sup>1</sup> Liu Zhichun<sup>1</sup> Ye Dong<sup>2</sup>

(1. School of Energy and Power Engineering, Huazhong University of Science and Technology, Wuhan 430074, China; 2. State Key Laboratory of Intelligent Manufacturing Equipment and Technology, Huazhong University of Science and Technology, Wuhan 430074, China)

### Abstract

**Significance** With the growing popularity of wireless sensors and wearable electronic devices in the IoT, the demand for in situ self-powered and flexible cooling technology has increased significantly. Flexible thermoelectric devices, capable of conforming intimately to curved heat sources, such as the human body, offer a unique solution by converting low-grade thermal energy from non-planar surfaces into electricity or localized cooling. These capabilities provide distinct advantages in applications such as self-powered wearable systems and thermal management of flexible electronics. The core strategy for realizing flexible thermoelectric devices involves integrating flexible thermoelectric materials or fabricating them into thin-film structures. Limited by materials and processing techniques, the first reported flexible thermoelectric device was not achieved until 2001, when a team from the Dresden University of Technology fabricated 50 pairs of 10- $\mu\text{m}$ -thick antimony (p-type) and bismuth (n-type) strips embedded in a flexible epoxy resin membrane. The device generated an output voltage of approximately 0.25 V under a temperature difference of 30 K. Current research on flexible thermodynamic devices can be broadly categorized into three main types: (i) high-performance flexible organic thermoelectric devices, (ii) thin-film-based flexible inorganic thermoelectric devices, and (iii) hybrid devices integrating rigid thermoelectric materials with flexible substrates. Over the past decade, flexible thermoelectric devices have achieved significant progress. For example, the device generated a maximum output power of 1.6 mW and maintained a temperature reduction of approximately 10 °C on skin, accelerating progress toward the practical application of flexible thermoelectric technologies.

**Progress** This review considers the flexible topological scheme of thermoelectric devices as the main focus and systematically examines

收稿日期:2026-03-18;修回日期:2026-04-07;录用日期:2026-04-21

责任编辑:田甜

基金项目:国家自然科学基金(52176007)和国家重点研发计划(2022YFB3803900)资助项目。(The project was supported by the National Natural Science Foundation of China (No. 52176007), National Key Research and Development Program of China (No. 2022YFB3803900).)



移动阅读

studies published over the past decade. A dimensionless characteristic length  $L/d$  was introduced for the thermoelectric arm, and its correlation with the figure of merit ( $ZT$ ) of the material was discussed. One-dimensional fiber-based devices primarily fall within the range of  $L/d > 10$ , whereas two-dimensional film-like devices typically exhibited  $L/d < 0.1$ . Three-dimensional bulk devices generally exhibited  $L/d$  values of  $0.1 - 10$ . Based on these findings, a classification framework for flexible thermoelectric devices was proposed according to the range of  $L/d$ . Meanwhile, one-dimensional fibrous devices demonstrated the best flexibility and wearing comfort, with normalized power density is only  $0.86 \mu\text{W}/(\text{cm}^2 \cdot \text{K}^2)$ . Two-dimensional film-like devices can be further categorized into thin-film, thick-film, and folding-type configurations, with maximum power density reaching  $30 \mu\text{W}/(\text{cm}^2 \cdot \text{K}^2)$ . Three-dimensional bulk devices achieved a steady output power of  $1.6 \mu\text{W}$  on skin, which is sufficient to power common sensors and wearable devices, demonstrating strong potential for practical engineering applications. Flexible cooling devices, however, remain in the early stages of development, and the maximum temperature reduction on skin can reach  $10^\circ\text{C}$ .

**Conclusion and Prospect** However, several bottlenecks in flexible thermoelectric devices must still be addressed. This review proposes the following directions for future optimization: (i) Developing three-dimensionally integrated device architectures, such as folding, curling, and multilayer stacking. (ii) constructing encapsulation structures with the ability to guide heat flow by directing it through the thermoelectric arms in a specific direction. (iii) selecting fatigue-resistant materials, such as flexible polyimides or silicone elastomers for encapsulation and designing stress-buffering structures to improve long-term operational reliability. (iv) advancing biomimetic designs in which the structure matches the Young's modulus of human skin and enhances moisture permeability, avoiding sudden and significant temperature drops in TEC, (v) improving performance evaluation system by considering key parameters, such as cooling capacity and coefficient of performance (COP), and developing accurate test methods and relevant standards (vi) integrating devices with efficient power management circuits and low-power energy storage units to support the stable operation of practical electronic devices.

**Keywords** flexible thermoelectric devices; wearable devices; flexible topology scheme; power generation performance; cooling performance

随着物联网无线传感器与可穿戴电子设备的普及,原位自供电与柔性冷却技术的需求日益迫切<sup>[1-2]</sup>。柔性热电器件能直接贴合人体等曲面热源,实现非平面热源低品位热能的发电<sup>[3]</sup>或曲面的快速制冷<sup>[4]</sup>,在可穿戴系统自供电、柔性电子器件冷却等领域展现出独特优势<sup>[5-6]</sup>。该类器件柔性化构筑的核心在于开发本征柔性的热电材料<sup>[7]</sup>或采用薄膜化制备工艺<sup>[8]</sup>,受限于材料与工艺的发展,直至2001年德累斯顿工业大学的团队基于前期成熟的微型气体传感器加工技术,制备了50对 $10 \mu\text{m}$ 厚度的铋条带(P型)与铋条带(N型)并将其嵌入柔性环氧树脂膜中,该器件在30 K温差下输出电压约0.25 V,成为了第一个报道的柔性热电器件<sup>[9]</sup>。此后,随着热电材料性能的不不断提升与微纳制造技术的进步,柔性热电的研究逐渐聚焦于结构创新与性能优化<sup>[10]</sup>。目前该类器件主要从3方面开展研究:高性能的柔性有机热电器件、薄膜化的柔性无机热电器件、柔性基底与刚性材料耦合的热电器件。近十年柔性热电器件取得显著进展,2023年清华大学<sup>[11]</sup>报道的器件在皮肤表面最大可产生1.6 mW的输出功率,2019年加利福尼亚大学<sup>[12]</sup>报道的器件可在皮肤表面保持约 $10^\circ\text{C}$ 的冷却温差,实用化进程不断加快。

鉴于柔性电子技术的持续演进,对自供电与冷却技术提出了更高要求,而柔性热电器件领域现有综述多集中于材料体系或工艺优化<sup>[13-15]</sup>,缺乏对器件

的柔性拓扑方案与性能间关联的总结<sup>[16]</sup>。因此,本文以热电器件的柔性拓扑方案为主线,对近十年的科研论文进行梳理,引入了热电臂的无量纲特征长度作为判断依据,将柔性热电器件划分为一维纤维、二维膜状、三维块体三大类。系统综述各类器件的性能与柔性结构,凝练了走向工程化应用所面临的瓶颈问题,并探讨了未来在提升器件性能、改善穿戴舒适性、实现系统化集成封装等方面的可行路径,以期对柔性热电技术的进一步研究和转化应用提供方向。

## 1 柔性热电发电器件

近十年柔性热电发电器件的报道已超过3 000篇,其应用主要围绕2个方面展开:1)作为传感单元,利用单对热电臂实现温差识别,并与压力、光强等传感机制耦合,构建多模态传感器;2)作为微功率电源,通过集成多对热电臂以产生足够的电能,为各类传感器与可穿戴设备持续供电。该技术在供电应用中覆盖多个领域,在计算与信号处理层面,可为时钟、数字信号处理器等提供能量;在环境感知领域,能够驱动气体、压力及温度传感器;在医疗保健方向可服务于起搏器、心电图监测前端等设备;在物联网系统中,还可支持无线传感节点等设备的运行。上述场景通常利用工业管道余热、轴承与发动机余热、太阳热能、人体皮肤热量进行发电。其中人体皮肤可视

为一个约 36 °C 的稳定热源,以约 25 mW/cm<sup>2</sup> 的热流密度向周围环境放热,在 20 °C 环境温度、自然对流条件下,器件贴附在人体皮肤表面时可建立约 5 K 的温差,足以产生 mV 量级的输出电压,这使得人体皮肤成为柔性热电发电器件最为常见的热源。而在贴附皮肤应用时,器件还需满足绝缘条件,避免皮肤受到电流刺激或产生汗液导致器件短路;同时应具备合适的热阻,避免热阻过低难以建立足够的温差,热阻过高导致皮肤发汗。

为了更好地梳理近十年柔性热电发电器件的发展,建立器件柔性、发电性能与适用场景之间的关联,本文定义无量纲特征长度  $L/d$  作为热电臂形态维度的表征参数。其中, $L$  为热电臂的长度, $d$  为横截面的特征尺寸,具体选取方式如图 1(a)~(c) 所示。以  $L/d$  为横坐标,材料  $ZT$  值为纵坐标绘制了近十年代表性器件的分布图,如图 1(d) 所示。可以发现一维纤维器件主要落于  $L/d > 10$  的范围内,二维膜状器件通常处于  $L/d < 0.1$  的范围内,三维块体器件的  $L/d$  介于 0.1~10,因此可根据  $L/d$  的范围定义柔性热电器件的划分方法。从物理意义角度,此时热电臂横截面积  $A \propto d^2$ ,因此对于常见的面外型器件,电阻  $R(\Omega)$ 、热阻  $R_{th}(K/W)$  可近似表示为:

$$R = \frac{\rho L}{A} \propto \frac{\rho \cdot L}{d \cdot d} \quad (1)$$

$$R_{th} = \frac{L}{\kappa A} \propto \frac{1}{\kappa d} \cdot \frac{L}{d} \quad (2)$$

式中: $\rho$  为材料电阻率, $\Omega \cdot m$ ;  $\kappa$  为材料热导率, $W/(m \cdot K)$ 。当 2 个物性参数及  $d$  保持不变时, $L/d$  与电阻、热阻成正比关系。然而各类器件中  $d$  与  $L/d$  是相互关联的:一维纤维器件  $L/d > 10$ ,  $d$  通常处于 10~300  $\mu m$  区间内,因此该类器件的电阻、热阻均相对较高;二维膜状器件  $L/d < 0.1$ ,  $d$  约为 0.1~10 mm,因此对于面外型结构的器件,其热阻、电阻均相对较低;三维块体器件的  $L/d$  介于 0.1~10,  $d$  通常为 0.5~4 mm,热阻和电阻处于中间水平。因此,在器件设计上,发电器件需要较高的热阻以建立足够的温差,同时应避免电阻显著升高导致输出功率降低;对于制冷器件,应优先考虑降低电阻以抑制焦耳热,通常倾向于  $L/d$  较小的面外型结构二维膜状器件。从材料维度观察,二维膜状和三维块体器件主要采用无机热电材料,其室温  $ZT$  值通常大于 0.1。其中二维膜状器件内热电臂的  $ZT$  值多集中于 0.6~0.9,最高可达约 1.5;三维块体器件多采用商业热电材料, $ZT$  值稳定在 0.9 附近。一维纤维器件则以有机材料为主,其  $ZT$  值通常低于 0.1,多数研究集中在  $10^{-3}$ ~ $10^{-2}$ 。值得注意的是,近期

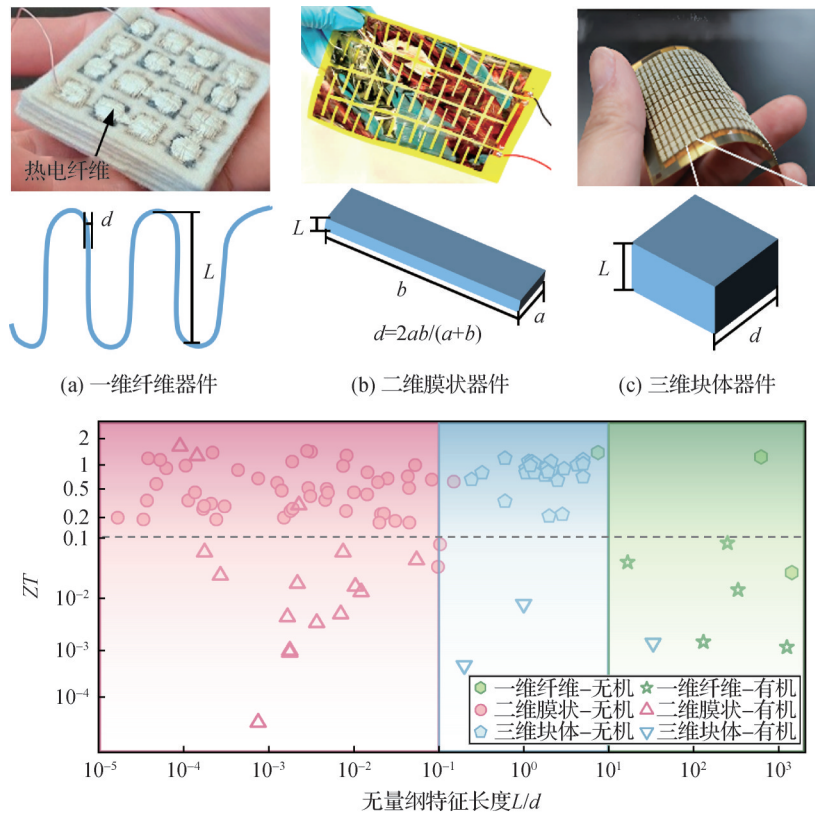


图 1 柔性热电发电器件的分类

Fig.1 Classification of flexible thermoelectric generators

中国科学院化学研究所狄重安研究员与朱道本院士团队<sup>[17]</sup>采用PDPPSe-12与聚苯乙烯构筑了具有不规则多级孔结构的聚合物材料,在343 K下测得ZT值高达1.64,这一突破性进展为高性能柔性有机热电材料的发展开辟了新路径。由于目前柔性热电器件的研究多聚焦于材料与器件层面,涉及能量管理与系统集成的报道相对有限,少数研究选择商用升压电路和电容进行能量管理,尚缺乏对启动电压、负载匹配及系统效率等关键参数的系统分析,因此本文基于图1的分类,仅从器件加工工艺、柔性结构、发电性能等方面,对3类柔性热电发电器件近十年的研究开展详细综述。

### 1.1 一维纤维器件

一维纤维器件主要由热电材料制成的纱线与柔性承载基底2部分组成,其中热电纱线作为核心功能单元,通过反复贯穿基底或缠绕于基底表面,在基底厚度方向形成冷端与热端平面,构建稳定温差并产

生电能。热电纱线的制备工艺与材料类型相关,无机热电材料通常采用拉伸<sup>[18]</sup>或加捻<sup>[19]</sup>制备成纱线,有机热电材料采用静电纺丝获得纤维原丝,再进行掺杂<sup>[20]</sup>或化学改性<sup>[21]</sup>提升热电性能。柔性承载基底不仅是器件的结构主体,也决定了器件的柔性与导热能力,因此根据承载基底,一维纤维器件可分为织物承载、其他聚合物承载2类。

织物承载类器件保留了织物的低热导率和优秀的柔性,代表性器件如图2(a)~(d)所示。H. Jang等<sup>[19]</sup>将交替沉积12层的纳米级Bi/Te膜捻成类似超晶格结构的热电纱线,再穿插于织物缝隙,4对纱线组成的器件在约100 K温差下产生67.4 mV电压。Zhang Ting等<sup>[18]</sup>则采用热拉拔工艺将碲化铋包裹在硅硼玻璃中得到直径400 μm的纱线,集成的器件柔性略有降低,在60 K温差下功率密度达2.34 mW/cm<sup>2</sup>。有机纱线制备的器件如图2(b)、(d)所示,He Xinyang等<sup>[22]</sup>将8根碳纳米管(CNT)/聚3,4-乙炔二氧噻吩混

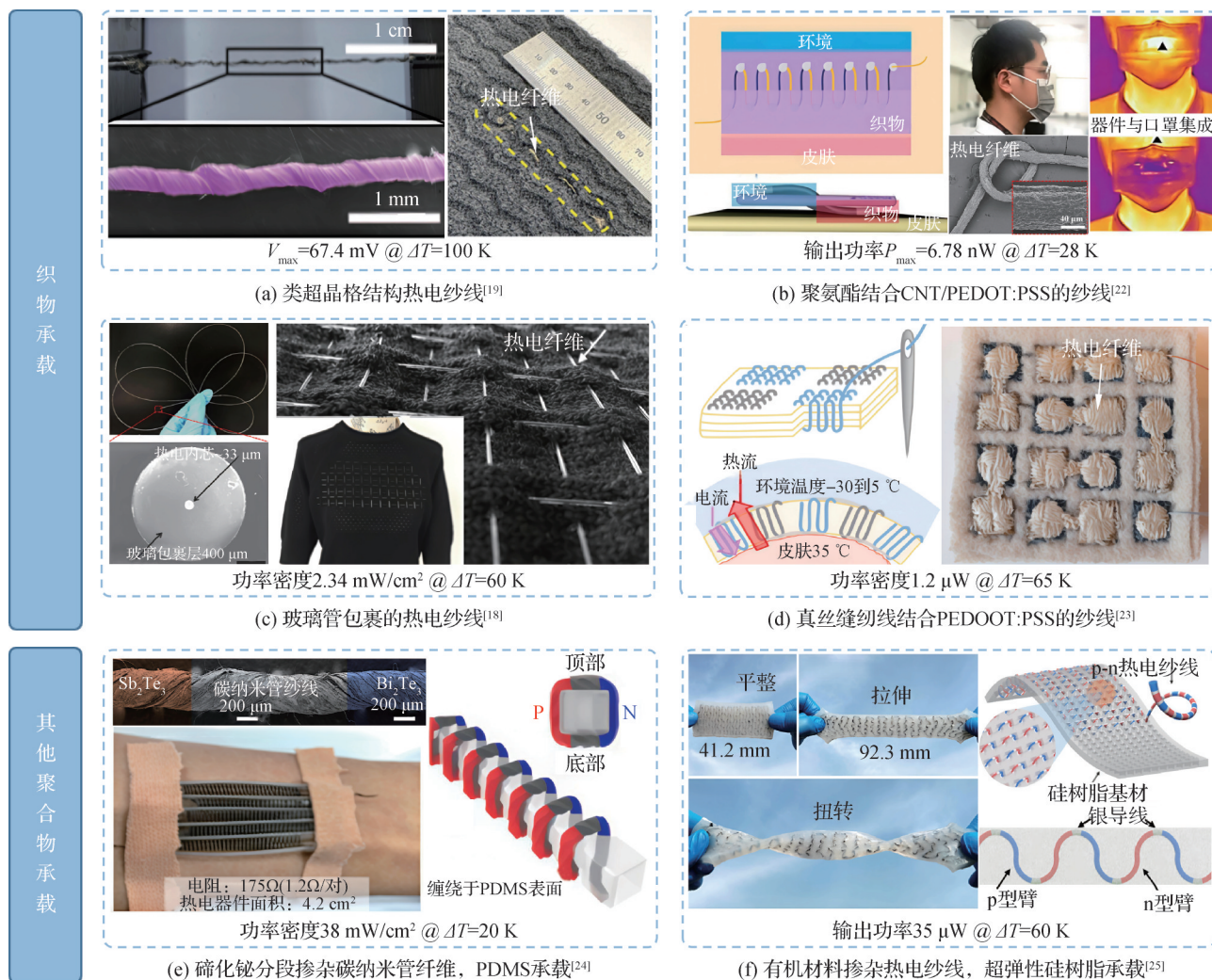


图2 一维纤维器件

Fig.2 One-dimensional fibrous device

合聚苯乙烯磺酸盐(PEDOT:PSS)掺杂的聚氨酯纱线集成在口罩内,28 K温差下输出功率为6.78 nW,最小识别温差为0.35 K。A. Lund等<sup>[23]</sup>以刺绣方式将133根PEDOT:PSS掺杂的真丝纱线集成在单个电极上,高热电臂密度使器件在65 K的温差下输出1.2  $\mu$ W。

其他聚合物承载类器件常以聚二甲基硅氧烷(polydimethylsiloxane, PDMS)、硅树脂等作为基底,其热导率略高于织物,柔性也相对较弱。如图2(e)、(f)所示,T. Lee等<sup>[24]</sup>在碳纳米管纱线上分段沉积碲化铋、碲化铋,再将其缠绕于PDMS表面进行组装,在20 K温差下功率密度为38  $\mu$ W/cm<sup>2</sup>。Wu Bo等<sup>[25]</sup>则以PEDOT:PSS、聚醚酰亚胺(PEI)掺杂的碳纳米管作为热电纱线,穿织于硅树脂基体中,并集成辐射散热以增强输出功率,在60 K的温差下达到35  $\mu$ W的输出功率。

除上述研究外,近年来还报道了许多新型高性能、高柔性的材料与器件。本文汇总的代表性文献的相关参数汇总于表S1(详见支撑材料),发现该类器件最高可达0.86  $\mu$ W/(cm<sup>2</sup>·K<sup>2</sup>)的归一化功率密度,但多数研究仅达10<sup>-3</sup>~10<sup>-2</sup>量级。总体而言,一维纤维器件在穿戴舒适性方面具有优势,但仍面临2方面挑战:当前一维纤维有机热电材料大多性能有限,导致器件输出功率通常偏低;织物难以与热源之间紧密贴合,温差利用率不足。因此,未来研究需着力开发更高性能的柔性热电材料,充分发挥纤维热电臂的可编织特性,通过优化纱线排布提升热电臂集成密度,从而提升温差利用率及器件输出性能。

## 1.2 二维膜状器件

二维膜状器件通常由微米级热电臂、电极以及薄膜状柔性基底(或封装材料)组成,这些结构使器件具备良好的变形能力,也实现了轻薄化与小型化,有利于与热源实现保形接触,适用于可穿戴设备。热电臂厚度直接影响其弯曲性能与制造工艺,据此可将热电臂分为2类<sup>[26]</sup>:厚度小于10  $\mu$ m的薄膜尺度热电臂,厚度大于10  $\mu$ m的厚膜尺度热电臂。此外,为在平面热源上建立更大温差、提升热源利用率,还发展出一种基于二维薄膜进行折叠的器件,将作为独立类型介绍。

### 1.2.1 薄膜器件

薄膜器件指热电臂厚度小于10  $\mu$ m的器件,兼具优异的柔性和较高的功率密度。其制备工艺分为2类:1)沉积技术,如磁控溅射<sup>[27]</sup>、电化学沉积<sup>[28]</sup>等;2)基于油墨或浆料的成膜技术,如印刷<sup>[29]</sup>、过滤<sup>[30]</sup>、旋涂<sup>[31]</sup>等。

沉积类工艺通常需借助掩模板实现图案化,其

精度与集成上限受到掩膜加工水平限制,利用光刻技术可显著提升热电臂集成度与器件性能。该类工艺中最常用的是磁控溅射技术,典型器件如图3(C)、(G)、(H)、(I)、(J)、(N)、(R)所示。Zhu Wei等<sup>[32]</sup>在PI(polyimide)基底上制备了厚度为2  $\mu$ m的12对碲化铋基热电臂,并采用放射状排列与太阳光吸收设计,在近100 K温差下功率为6.5  $\mu$ W。Wang Xizu等<sup>[33]</sup>利用PEDOT:PSS与氧化铜锡制备了近透明器件,在80 K温差下功率密度为2.22 mW/cm<sup>2</sup>。Wang Yaling等<sup>[34]</sup>采用Bi<sub>2</sub>Te<sub>3</sub>、Sb<sub>2</sub>Te<sub>3</sub>与Te共沉积工艺,结合氮化硼改性PDMS,制成手腕穿戴的自供电传感器,输出功率密度达2.52  $\mu$ W/cm<sup>2</sup>。Huang Xiaolan等<sup>[35]</sup>与Lei Yan等<sup>[36]</sup>分别通过退火硒化与水相硒化反应制备了Cu<sub>2</sub>Se与 $\beta$ -Ag<sub>2</sub>Se薄膜器件,在38 K与60 K温差下功率密度分别为58.07  $\mu$ W/cm<sup>2</sup>与5.44  $\mu$ W/cm<sup>2</sup>。Chen Yuexing等<sup>[37]</sup>采用类似工艺,并在Ag<sub>2</sub>Se膜表面引入保护层以抑制弯曲开裂,器件在42 K温差下功率密度为6.5 mW/cm<sup>2</sup>。次年,Tan Ming等<sup>[38]</sup>制备了ZT值分别为1.44、1.39的N型Bi<sub>2</sub>Te<sub>2.7</sub>Se<sub>0.3</sub>薄膜和P型Bi<sub>0.5</sub>Sb<sub>1.5</sub>Te<sub>3</sub>薄膜,其性能与Mao Dasha等<sup>[39]</sup>报道的Bi<sub>0.4</sub>Sb<sub>1.6</sub>Te<sub>3</sub>薄膜(ZT=1.4)相当。该研究在30×30 mm<sup>2</sup>的基板上集成162对热电臂,并采用倒装键合工艺封装,实现4.36  $\mu$ W/(cm<sup>2</sup>·K<sup>2</sup>)的归一化功率密度,贴肤时可产生365 mV的电压。

其他沉积工艺制备的器件如图3(B)、(F)、(L)所示。J. Na等<sup>[40]</sup>采用脉冲电化学沉积法在AFS胶带上制备厚度为2~3  $\mu$ m的热电臂,12 K温差下器件输出功率为56 nW。V. Karthikeyan等<sup>[41]</sup>则采用物理气相沉积方法制备厚度为100 nm的SnTe和PbTe薄膜。Zhang Jian等<sup>[42]</sup>结合光刻和脉冲电镀技术在3  $\mu$ m的PI基底上制备了仅0.0246 g的超薄超轻器件,在29.9 K的温差下输出功率为4.66 mW,功率密度为16.0 mW/cm<sup>2</sup>,对应单位质量功率为189 mW/g。

基于油墨或浆料的成膜技术在图案化方面灵活性更高,但加工精度相对较低,制备的器件如图3(A)、(D)、(E)、(M)、(O)、(P)、(Q)所示。N. Toshima等<sup>[43]</sup>采用滴铸法在PI基底上制备了三元复合薄膜,在100 K温差下器件输出3.88  $\mu$ W。Lu Yao等<sup>[44]</sup>采用类似方式制备了厚度为3~5  $\mu$ m的Te/PEDOT:PSS/Cu<sub>7</sub>Te<sub>4</sub>三元纳米复合薄膜。油墨印刷工艺也较为常见,Liu Yan等<sup>[45]</sup>采用该技术制备Ag<sub>2</sub>Se薄膜并集成光热/辐射冷却涂层,器件达1.1  $\mu$ W/(cm<sup>2</sup>·K<sup>2</sup>)的归一化功率密度。M. Saeidi-Javash等<sup>[46]</sup>结合快速光子烧结在PI基底上制备了厚度为1.45  $\mu$ m的Bi<sub>2</sub>Te<sub>2.7</sub>Se<sub>0.3</sub>薄膜,器件功率密度为2.7 mW/cm<sup>2</sup>。Du Jingjie等<sup>[47]</sup>结

合热压烧结制备了  $\text{Ag}_{2.1}\text{Te}$  薄膜, 器件归一化功率密度为  $0.9 \mu\text{W}/(\text{cm}^2 \cdot \text{K}^2)$ 。在过滤成膜方面, Dai Xu 等<sup>[48]</sup>结合自动激光制造法得到的光电-热电器件, 在 40 K 温差下功率密度为  $0.32 \mu\text{W}/\text{cm}^2$ 。此外, 有研究通过旋涂和紫外曝光构建有机超晶格薄膜<sup>[31]</sup>, 单个周期由 6 nm 的 PDPPSe-12 和 4 nm 的 PBTTT 及中间 4 nm 的过渡层组成。器件采用  $1.8 \mu\text{m}$  的薄膜制备, 归一化密度为  $1.12 \mu\text{W}/(\text{cm}^2 \cdot \text{K}^2)$ 。

除上述主流工艺外, W. B. Han 等<sup>[49]</sup>采用光刻和湿法蚀刻技术得到硅纳米线热电臂, 结合可拉伸、可生物降解的纤维膜及光热设计, 在 20 K 温差下功率

密度为  $40 \mu\text{W}/\text{cm}^2$ 。

除上述研究外, 近年来还报道了一些具有良好性能的薄膜器件。代表性文献的相关参数汇总于表 S2 (详见支撑材料), 其中器件最高可达  $16.0 \mu\text{W}/(\text{cm}^2 \cdot \text{K}^2)$  的归一化功率密度, 其他研究主要在  $1 \sim 4 \mu\text{W}/(\text{cm}^2 \cdot \text{K}^2)$  区间内。虽然当前多数器件中集成的热电臂对数较少, 输出功率多在纳瓦至微瓦级, 但受益于超薄结构赋予的极小的截面积与体积, 仍表现出较高的功率密度, 应用前景广阔。此类器件目前仍存在电阻过大、封装工艺不完善、难以大面积快速制造等挑战, 未来需聚焦于这些问题。



图 3 近十年薄膜器件的发展历程

Fig.3 Development of thin-film devices in the last decade

### 1.2.2 厚膜器件

厚膜器件是指热电臂厚度介于  $10 \sim 500 \mu\text{m}$  的器件, 由于热电臂厚度增加器件柔性降低, 但机械强度与结构稳定性提升<sup>[50]</sup>; 同时器件电阻降低、热阻升高, 有利于在相同热源条件下建立更大温差, 获得更高的输出功率。图 4 展示了近十年的代表性器件, 其热电臂的制备工艺主要分为 2 类: 1) 基于油墨或浆料的成膜技术, 如丝网印刷<sup>[51]</sup>、过滤<sup>[52]</sup>、刷涂<sup>[53]</sup>等; 2) 三维材料减薄技术, 如切割<sup>[54]</sup>、胶带剥离<sup>[8]</sup>、轧制<sup>[55]</sup>等。

基于油墨或浆料的成膜技术在厚膜器件制备中应用广泛, 其中印刷类工艺尤为常见, 相关器件如图 4(A)、(B)、(C)、(E)、(G)、(J)、(K)、(R) 所示。D. Madan 等<sup>[56]</sup>采用喷墨印刷技术在双层 F-PCB 板上制备了厚度为  $100 \mu\text{m}$  的热电臂, 器件在 20 K 温差下输出功率为  $33 \mu\text{W}$ 。Y. S. Jung 等<sup>[57]</sup>沿用类似工艺, 集成光热涂层与聚对二甲苯保护层后在 1.5 倍太阳光强下输出功率为  $4.44 \mu\text{W}$ 。J. Peng 等<sup>[58]</sup>结合对辊工艺得到宽度约为  $500 \mu\text{m}$ 、厚度为  $100 \mu\text{m}$  的热电膜,

采用5对热电臂组装的2种器件在约70 K温差下输出功率分别为26.2 nW与3.4 nW。Y. S. Kim等<sup>[59]</sup>采用油墨打印、退火、紫外光照射工艺,制备了无色的热电臂,器件可达 $0.325 \mu\text{W}/(\text{cm}^2 \cdot \text{K}^2)$ 的归一化功率密度。S. H. Park等<sup>[60]</sup>将浆料刷涂、烧结得到柔性器件,在50 K温差下功率密度为 $2.43 \text{ mW}/\text{cm}^2$ 。T. Varghese等<sup>[61]</sup>通过丝网印刷制备了掺入碲颗粒的 $\text{Bi}_{0.4}\text{Sb}_{1.6}\text{Te}_3$ 厚膜器件,在80 K温差下功率密度达 $18.8 \text{ mW}/\text{cm}^2$ 。D. Lee等<sup>[62]</sup>采用油墨滴铸法制备自支撑热电臂,与碳纳米管薄膜组装的器件在35 K温差下功率密度为 $0.418 \mu\text{W}/\text{cm}^2$ 。Liu Jinzhuo等<sup>[63]</sup>则以纯碳纳米管制备热电臂,结合光热涂层的器件在1个太阳光强下功率密度为 $32 \mu\text{W}/\text{cm}^2$ 。

过滤成膜工艺同样应用较多,相关器件如图4(D)、(F)、(H)所示。Wang Liming等<sup>[64]</sup>通过真空过滤制备 $\text{TiS}_2/\text{C}_{60}$ 复合薄膜,器件在20 K温差下功率密度为 $168 \mu\text{W}/\text{cm}^2$ 。Ding Yufei等<sup>[65]</sup>以相同工艺在尼龙基底上制备 $\text{Ag}_2\text{Se}$ 热电臂,组装的器件在30 K温差下功率密度为 $230 \mu\text{W}/\text{cm}^2$ 。Fan Jueshuo等<sup>[66]</sup>采用单臂碳纳米管与SnSe制备厚度为 $21 \mu\text{m}$ 的膜,封装后的器件在60 K温差下输出 $1.38 \mu\text{W}$ 。

其他成膜技术制备的器件如图4(M)、(O)所示。Liu Yuanmeng等<sup>[67]</sup>采用超声分散技术,以 $\text{NaBH}_4$ 掺杂碳纳米管油墨并进行铸膜、冷压处理,组装的器件在40 K温差下功率密度为 $2.996 \mu\text{W}/\text{cm}^2$ 。Li Wenhui等<sup>[68]</sup>则通过超声分散、烘干得到厚度约为 $15 \mu\text{m}$ 的复合薄膜,相同温差下功率密度为 $173 \mu\text{W}/\text{cm}^2$ 。

三维材料减薄技术通过物理方法将块体材料减薄至 $10\sim 500 \mu\text{m}$ ,代表性器件如图4(I)、(L)、(N)、(P)、(Q)所示。Yang Qingyu等<sup>[5]</sup>将 $\text{AgCu}(\text{Se}, \text{S}, \text{Te})$ 伪三元固溶体铸锭切割并打磨为厚度为 $100 \mu\text{m}$ 的热电臂,制备的多种填充率器件最优性能可达 $30 \mu\text{W}/(\text{cm}^2 \cdot \text{K}^2)$ 的归一化功率密度。在胶带剥离方面, Lu Yao等<sup>[8]</sup>将单晶 $\text{Bi}_{0.5}\text{Sb}_{1.5}\text{Te}_3$ 和 $\text{Bi}_2\text{Te}_3\text{Se}_{0.3}$ 剥离为 $12 \mu\text{m}$ 的厚膜,组装器件在60 K温差下功率密度为 $32.1 \text{ mW}/\text{cm}^2$ 。Deng Tingting等<sup>[69]</sup>将温度梯度法生长的 $\text{Cu}_{0.005}\text{SnSe}_{1.95}\text{Br}_{0.05}$ 单晶剥离得到厚度约为 $150 \mu\text{m}$ 的膜,所得器件在30 K温差下功率密度为 $7.84 \mu\text{W}/\text{cm}^2$ 。在轧制工艺中, Ding Wenjun等<sup>[70]</sup>通过多次热轧将 $\text{Ag}_2\text{Se}$ 从 $523 \mu\text{m}$ 减薄至 $36 \mu\text{m}$ ,器件在69 K温差下功率密度达 $16.7 \text{ mW}/\text{cm}^2$ 。Wang Yuechu等<sup>[71]</sup>则利用冷轧与退火处理,使具有室温塑性的 $\text{Ag}_2\text{Te}_{0.6}\text{S}_{0.4}$

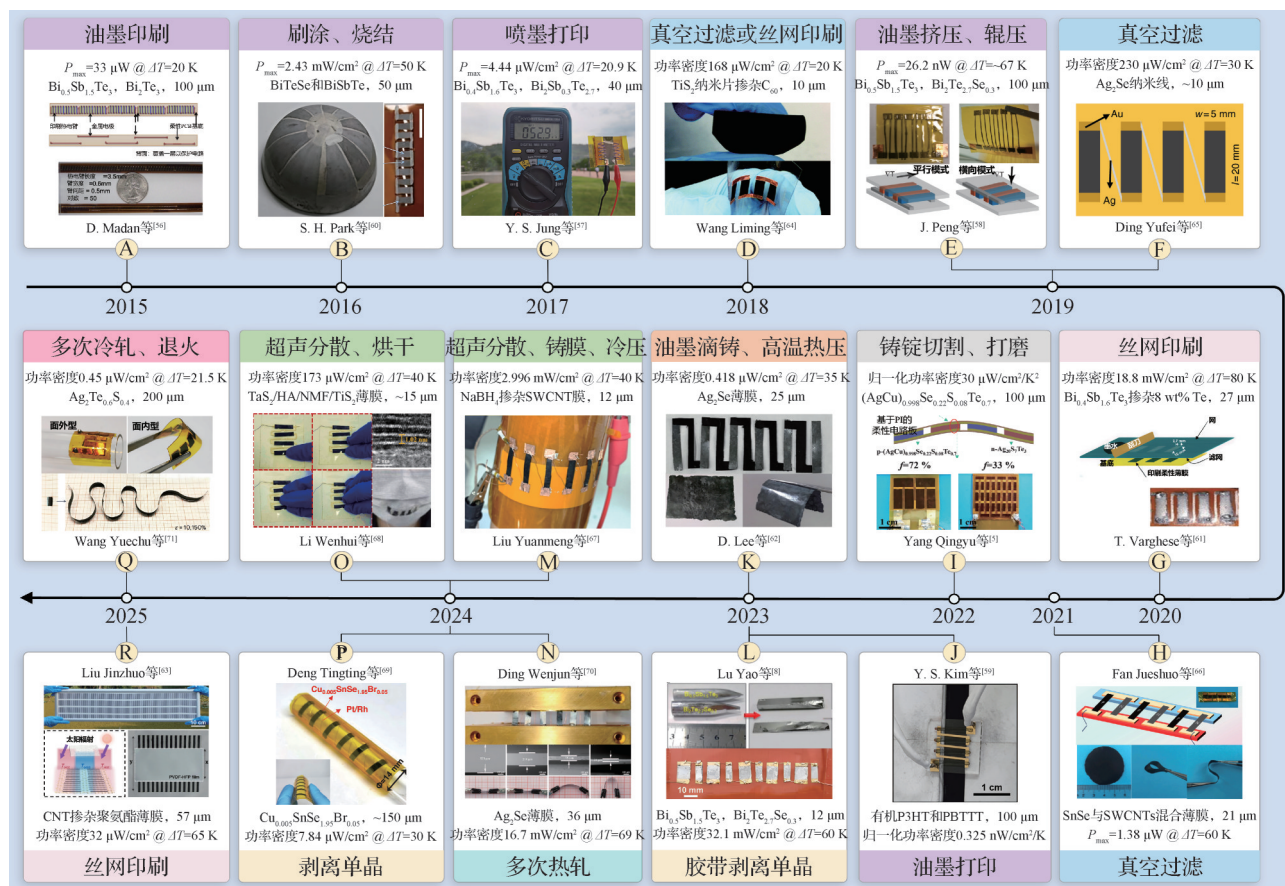


图4 近十年厚膜器件的发展历程

Fig.4 Development of thick-film devices in the last decade

粒子展现出 10~150% 的超高延展性,以厚度为 200  $\mu\text{m}$  的膜制备面内型器件,在 21.5 K 的温差下功率密度为 0.45  $\mu\text{W}/\text{cm}^2$ 。

更多厚膜尺度器件的性能参数汇总于如表 S3 (详见支撑材料),器件最高可达 30  $\mu\text{W}/(\text{cm}^2\cdot\text{K}^2)$  的归一化功率密度,无机材料制备的器件处于 0.012~8.917  $\mu\text{W}/(\text{cm}^2\cdot\text{K}^2)$  区间内,有机材料制备的器件仅为  $10^{-5}$ ~ $10^{-3}$  量级。总体而言,厚膜尺度器件在输出功率方面具备优势,且丝网印刷、轧制等工艺有利于规模化制备。然而,该类器件仍面临两大挑战:1)多数器件采用面内型结构,虽然相较同类的薄膜尺度器件可以建立更高的温差,但对人体皮肤等平面热源的利用率仍较低,需进一步优化材料性能与器件构型;2)厚度增加导致柔性下降,在较小的弯曲半径下易引发开裂或界面失效,需要发展有效的封装策略以提升其可靠性与环境适应性。

### 1.2.3 折叠器件

折叠器件以二维热电薄膜为基础,通过将热电臂插入基底<sup>[72-73]</sup>,或采用折叠<sup>[74]</sup>、卷曲<sup>[75]</sup>等方式构建具有复杂空间拓扑的器件。该类设计一方面可重构热输运路径,延长热流在热电臂内传输距离,提升温差利用率<sup>[76]</sup>;另一方面,能在有限投影面积内集成更多热电臂,显著提升输出功率密度。依据组装方式,该类器件主要分为翅片型与非翅片型 2 类。

翅片型器件将二维膜状热电臂或器件垂直竖立于同一平面,形似基板上的翅片阵列,从而使热量竖直输运。该类器件结构简单,在对流换热的场景下具有更优的输出功率,相关器件如图 5(a)~(d)所示。Zhou Qing 等<sup>[77]</sup>将有机热电薄膜对垂直插入硅橡胶基底并用银膏连接,在 14 K 的温差下功率密度为 0.18  $\mu\text{W}/\text{cm}^2$ 。Chen Wenyi 等<sup>[1]</sup>先制备高性能薄膜器件,再切割并折叠热电臂形成竖直翅片结构,可达 3  $\mu\text{W}/(\text{cm}^2\cdot\text{K}^2)$  的归一化功率密度。另有学者将电极设计为可折叠的三角形结构<sup>[78]</sup>,当电极压紧或平铺时实现结构切换,70 K 温差下输出功率密度为 337.4  $\mu\text{W}/\text{cm}^2$ 。Zeng Chongyang 等<sup>[79]</sup>采用剪纸工艺与两次折叠,并耦合了大面积铜层散热,所制备器件达到了 2  $\mu\text{W}/(\text{cm}^2\cdot\text{K}^2)$  的归一化功率密度。

翅片型结构以外的器件归为非翅片型器件,其通常具有更小的体积和更高的热电臂密度,代表性器件如图 5(e)~(h)所示。Zhang Dehui 等<sup>[76]</sup>将条带状的热电薄膜在界面处弯折并交替穿过厚度为 4 mm 的柔性硅树脂基板,在 60 K 温差下功率密度为 234.3  $\mu\text{W}/\text{cm}^2$ 。Tao Xudong 等<sup>[80]</sup>将含 25 对热电臂的薄膜器件沿着短边卷曲成圆柱状单元,再将 9 个单元串联并

嵌入 PDMS,形成的腕带穿戴时产生 90 mV 的电压。Wu Bo 等<sup>[81]</sup>采用三级折叠封装策略,以碳纳米管薄膜、绝缘层及铜箔制备器件,并采用 PI 封装,该器件在 38.9 K 温差下输出功率密度 140.9  $\mu\text{W}/\text{cm}^2$ 。Yuan Xinjie 等<sup>[2]</sup>则利用电极两端的铜柱引导热流垂直-横向-垂直传输,在 12 K 温差,1.5 m/s 风速下功率密度达 1.15  $\mu\text{W}/\text{cm}^2$ 。

除上述研究以外,部分还探索了具有高热电臂密度的新型结构设计,相关代表性器件的性能汇总于表 S4 (详见支撑材料),该类器件最高可达 3  $\mu\text{W}/(\text{cm}^2\cdot\text{K}^2)$  的归一化功率密度,其他研究多为  $10^{-4}$ ~ $10^{-1}$  量级。折叠器件通过重构热输运路径与提升热电臂集成度,显著增强了在皮肤等平面热源上温差利用率和输出功率。然而,当前多数设计以增大体积、牺牲柔性为代价,在可穿戴性与结构紧凑性方面仍需改善。未来研究应保持输出功率的同时着力于器件轻薄化、柔性化,以满足可穿戴需求。

### 1.3 三维块体器件

三维块体器件由块体热电臂、电极以及柔性基底或填充材料组成。根据材料特性与工艺差异,块体热电臂主要分为柔性和刚性 2 类。柔性块体热电臂包括热电海绵<sup>[7]</sup>、热电粘土<sup>[82]</sup>、气凝胶<sup>[83]</sup>等,制备过程通常较为复杂;刚性块体热电臂多直接使用商用热电颗粒,仅需选择合适尺寸即可组装器件,且材料性能普遍优于柔性材料,因此得到更多学者的关注。

虽然刚性热电臂本身不具备柔性,但通过柔性基底或封装材料的形变使器件具备柔性。根据构筑策略可将该类器件分为 2 种:1)采用柔性基底,称为非填充型器件。该类器件热电臂周边为热导率极低的空气<sup>[84]</sup>,有利于将热流集中在热电臂,提升热量利用效率;但器件四周缺少封装,不具备防水能力。2)采用柔性填充材料封装,称为填充型器件。该类器件将热电臂封装于填充材料内部<sup>[85-86]</sup>,具备良好的防水能力。部分设计借助填充材料实现结构自支撑,避免基板带来的温差损失;然而填充材料的导热系数高于空气,不利于热流在热电臂两端的集中。

非填充型器件的典型结构如图 6(a)、(b)所示,一般采用 PI 或 PDMS 基底实现器件的柔性。T. Sugahara 等<sup>[87]</sup>侧重于热电臂填充率的提升,在 50×50 mm<sup>2</sup> 的 PI 基底上集成 125 对碲化铋基热电臂,填充率达 58.33%,在 105 K 的温差下实现 158 mW/cm<sup>2</sup> 的输出功率密度。Yuan Jinfeng 等<sup>[11]</sup>侧重于大规模集成,制备了含 448 对热电臂的器件,但填充率仅为 7%,佩戴在人体腿部并在 9 km/h 奔跑条件下,输出功率约为 1 600  $\mu\text{W}$ ,功率密度为 0.469  $\mu\text{W}/\text{cm}^2$ 。另有

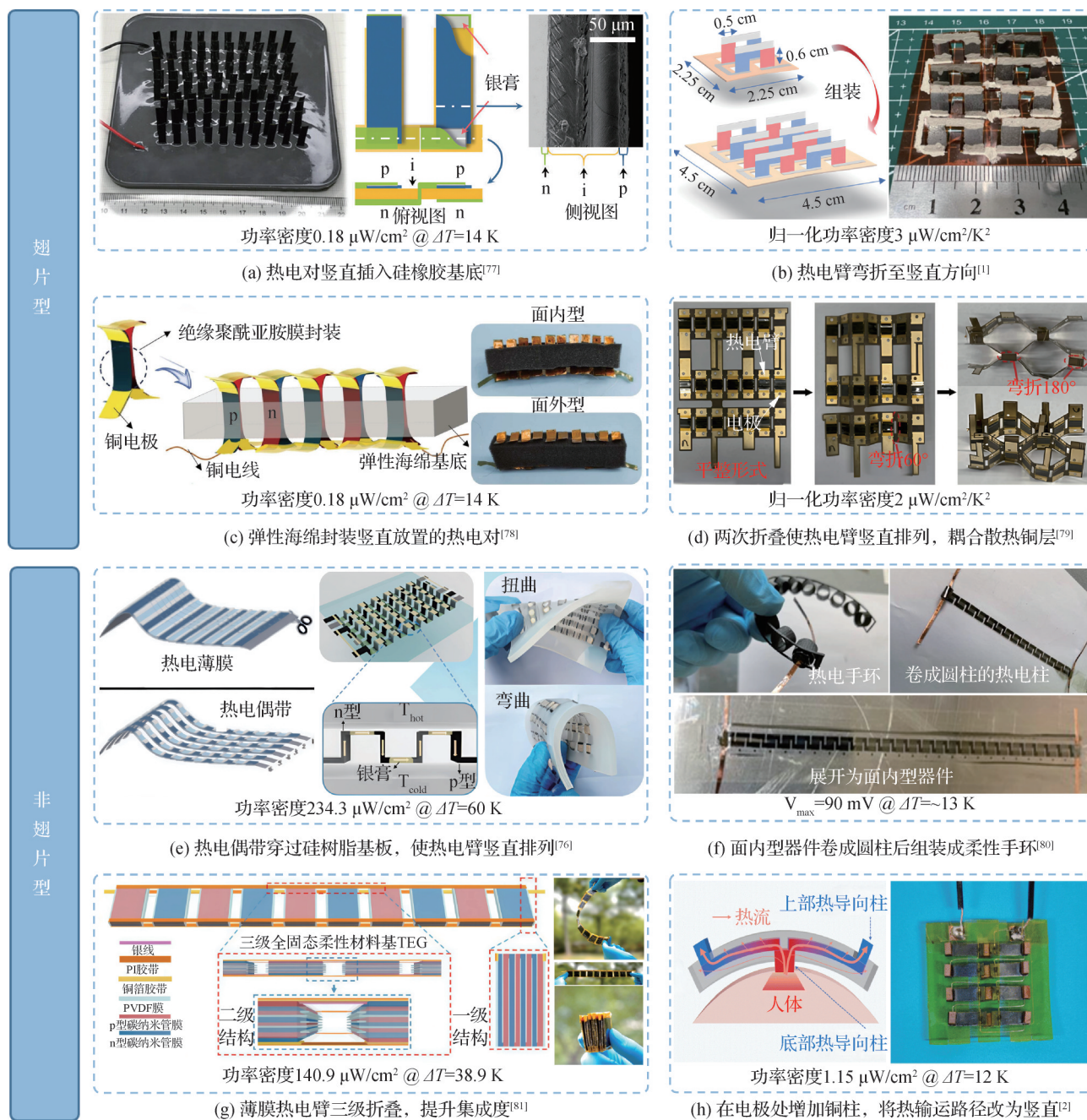


图5 折叠器件

Fig.5 Devices obtained by folded film

研究在器件两端集成辐射散热层<sup>[88]</sup>或光吸收涂层以提升性能,如 Y. Jung 等<sup>[89]</sup>同时结合两种涂层,在正午功率密度达到  $18.59 \mu\text{W}/\text{cm}^2$ 。

填充型器件通常采用 PDMS、铂金硅胶 (Ecoflex) 等柔软且富有弹性的材料进行封装。根据集成的散热结构及电极形式,该类器件可进一步细分为不可拉伸型与可拉伸型 2 类。

不可拉伸型器件的典型结构如图 6(c)、(d) 所示。其拉伸能力受限于电极形态,但提升发电性能的方式不同。M. Jeong 等<sup>[90]</sup>采用骨状电极扩大底部吸光层面积,顶部连接泡沫铜散热器以增大温差,在

体热与阳光共同作用下温差  $10.9 \text{ K}$ ,功率密度  $15.33 \mu\text{W}/\text{cm}^2$ 。S. Jung 等<sup>[91]</sup>以压铸白糖制成的多孔方糖作为模具,制备出导热系数仅为  $0.08 \text{ W}/(\text{m}\cdot\text{K})$  的多孔 PDMS 海绵作为填充材料,该器件置于手臂上时输出电压为  $5 \text{ mV}$ ,输出功率密度为  $12.1 \mu\text{W}/\text{cm}^2$ 。

可拉伸型器件的典型结构如图 6(e)~(h) 所示,通常以蛇形电极保证电连接的稳定性,柔性来源于封装材料的弹性或设计的可拉伸结构。图 6(e)、(f) 中器件通过结构优化提升发电性能。Y. Han 等<sup>[92]</sup>将封装材料设计为网格状,使空气填充热电臂周围区域,并集成可拉伸热沉以增强两端温差,在  $10 \text{ K}$  温差

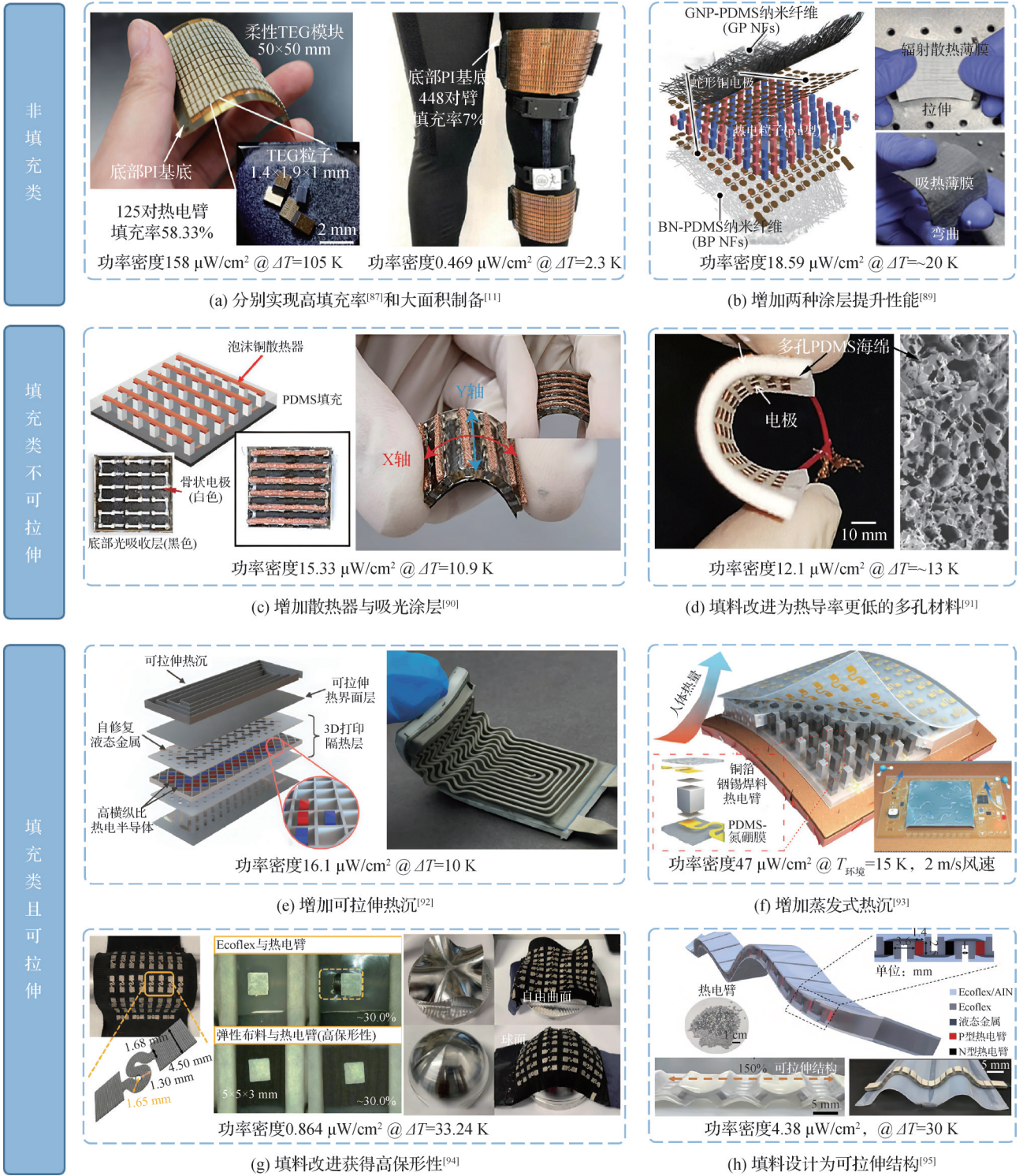


图6 三维块体器件

Fig.6 Three-dimensional block devices

下功率密度达到 16.1 μW/cm<sup>2</sup>。An Zijia 等<sup>[93]</sup>则在 Ecoflex 填料中掺入 25% 的空心玻璃微珠,将导热系数降至 0.1 W/(m·K),结合蒸发式热沉,在 15 °C 环境温度及 2 m/s 风速条件下,功率密度达到 47 μW/cm<sup>2</sup>。图 6(g)、(h) 中器件则侧重于柔性设计的创新。Hou Yue 等<sup>[94]</sup>采用弹性织物和导电聚酯纤维布作为基底与电极,在 30% 拉伸应变下仍保持良好的贴合性,于

33.24 K 温差时输出功率密度为 0.864 μW/cm<sup>2</sup>。Jin Junfeng 等<sup>[95]</sup>在 Ecoflex 填料中构筑凹槽结构,使器件在宏观上具备柔性可拉伸能力,该器件在 30 K 温差下的功率密度为 4.38 μW/cm<sup>2</sup>。

更多三维块体器件的性能参数与柔性构筑方法汇总于表 S5 (详见支撑材料),器件最高可达 14.33 μW/(cm<sup>2</sup>·K<sup>2</sup>) 的归一化功率密度,其他器件常处于

0.01~7.3  $\mu\text{W}/(\text{cm}^2\cdot\text{K}^2)$  区间内。总体而言,基于三维块体热电臂制备的器件工艺相对简单,在输出功率方面优势显著。部分研究已将器件集成至传感系统内,工程应用潜力强。但该类器件普遍存在厚度较大、体积笨重、穿戴贴合性欠佳的问题,未来研究应在保持输出性能的同时,进一步在轻薄化与穿戴舒适性等方面寻求突破,并完善与能量管理、耗能器件的集成,推进器件的工程化应用。

## 2 柔性热电制冷器件

柔性热电制冷器件是指通入电流后能够产生净制冷温差或净制冷量,且具备弯曲能力的器件。符合该定义的首个器件于2017年被报道,该器件贴附皮肤时最大冷却温差为3.8 K<sup>[96]</sup>。柔性热电制冷器件通常由二维膜状或三维块体的热电臂、电极以及柔性基底或封装材料组成。与发电器件类似,热电臂的无量纲特征长度  $L/d$  同样显著影响器件柔性与性能,因此将该类器件分为三维块体<sup>[97]</sup>与二维膜状<sup>[98]</sup>2类。其中,三维块体器件面向个人可穿戴冷却,如贴附于人体皮肤的局部冷却装置;二维膜状器件则适用于柔性电子设备的冷却,如柔性芯片、智能眼镜、可折叠显示屏等散热场景。

三维块体制冷器件通常选用商用热电颗粒或小型商用器件作为制冷单元,以柔性封装材料实现整体柔性,部分器件会耦合热沉以维持稳定的制冷能力。未耦合热沉的器件如图7(A)、(C)、(E)、(F)、(K)所示。H. Park等<sup>[96]</sup>将研磨烧结工艺制备的热电臂与酚醛树脂、柔性导线组装成器件,P型、N型材料  $ZT$  值分别约为0.98、0.64。该器件通入3 A电流时最大冷却功率密度为79.87  $\text{mW}/\text{cm}^2$ ,贴附皮肤并通入1.27 A电流可使皮肤降温3.8 K。S. Hong等<sup>[12]</sup>将  $ZT$  值约为0.71的块体热电臂嵌入掺杂AlN的Ecoflex中,集成到衣物后,在36 °C环境下通入160 mA电流可实现10 K冷却温差。Yang Mingkun等<sup>[99]</sup>采用液态金属GaIn替代部分电极,并以PDMS逐层封装,该器件在30 °C环境温度通入1 A电流时冷却温差为7.4 K。Xu Yunhe等<sup>[100]</sup>以  $ZT$  值超过1.1的  $\text{Bi}_2\text{Te}_3$  粒子、Ecoflex与液态金属构建器件,在5 V电压下可于300 s内保持7.8 K的稳定冷却温差。Sun Xiaolong等<sup>[101]</sup>选用自修复封装材料,开发了单级与两级的柔性制冷器件,在0.8 A电流下,最大制冷温差分别为3.9 K与6.2 K。

为有效管理热端堆积的热量,如图7(D)、(H)、(I)所示的器件集成了热沉。J. Choi等<sup>[102]</sup>将4个小型TEC串联后封装在硅树脂中,并耦合含相变材料

的柔性热沉,器件在0.5 W输入功率下可实现5小时内1.5 °C的冷却温差。Wu Bo等<sup>[103]</sup>将商用热电臂夹入PI薄膜后形成热电单元,再插入硅酮弹性体形成翅片结构,器件在2 m/s风速与0.5 A电流下可获得4 K的制冷温差。Zhang Pengxiang等<sup>[104]</sup>则将刚性热电臂与多孔水凝胶结合,采用发汗冷却技术处理热端热量,制备的电子皮肤在40 °C环境温度下可维持35 °C长达4.2 h。

二维膜状制冷器件在设计上更注重冷量的集中,倾向于采用如图7(G)、(J)所示的放射状结构,Li Chengjun等<sup>[105]</sup>引入Ag/PZT/PVDF/热电材料的夹层铁电极化结构,在3 kV极化电压下热电薄膜功率因子为20.8  $\mu\text{W}/(\text{cm}^2\cdot\text{K}^2)$ ,通入10 mA工作电流时净制冷温差达2.4 K。Dong Guoying等<sup>[106]</sup>通过磁控溅射与液相Te辅助生长制备了高性能薄膜,常温下P型材料  $ZT$  值可达1.47,N型材料  $ZT$  值为1.02。针对局部热点消除设计的放射状器件,在300 K真空环境中最大制冷温差为5.3 K,353 K环境下可提升至8.01 K。平行结构的器件如图7(B)、(L)所示,Hou Weikang等<sup>[107]</sup>采用刷涂与热压固化工艺制备了150  $\mu\text{m}$ 厚的  $\text{Bi}_{0.5}\text{Sb}_{1.5}\text{Te}_3$  薄膜,材料在300 K时功率因子达8.4  $\mu\text{W}/(\text{cm}^2\cdot\text{K}^2)$ ,器件在0.06 A电流下可以建立6.2 K的温差。Ke Shaoqiu等<sup>[108]</sup>利用强磁性(Fe)与弱磁性( $\text{Fe}_3\text{O}_4$ )纳米颗粒增强性能,通过丝网印刷制备的材料最大面内功率因子为28.7  $\mu\text{W}/(\text{cm}^2\cdot\text{K}^2)$ ,制备的器件在热端314 K时,制冷温差分别为2.5 K与0.7 K。

更多柔性热电制冷器件的参数汇总于表S6(详见支撑材料)。总体而言,当前柔性热电制冷器件的研究仍处于起步阶段,研究重点多集中于材料加工与器件制备。在性能表征方面,通常仅测试器件两端温差以表征性能,难以全面反映器件实际制冷能力。尤其对于二维膜状器件,其制冷量较小,传统测试方法难以精准测量;其厚度很薄,传统性能测试台难以直接测定冷热端温度。未来研究应增加最大制冷量、冷却热流密度、功耗及COP(coefficient of performance,性能系数)等参数的测量,并发展基于热真空测试的薄膜型器件精准测试方法,以完善器件评价体系。在结构设计方面,当前结构容易损失制冷量,削弱制冷温差。因此,针对三维块体器件,需要进一步降低基板寄生热阻并优化填充材料的导热特性;对于二维膜状器件,需要适当增加电极、热电臂的厚度,在降低电阻、抑制焦耳热的同时提升热阻,防止热端热量回流至冷端抵消制冷量。在长期工作方面,多数器件缺乏有效的热沉设计,限制了持续制冷时长,难以满足可穿戴场景的长期需求。因

此,未来研究需完善器件形成测试与评价体系,在低热阻封装设计、高效柔性散热以及器件级热电协同

优化等方面进行深入探索,以实质性提升其制冷效率与实用价值。

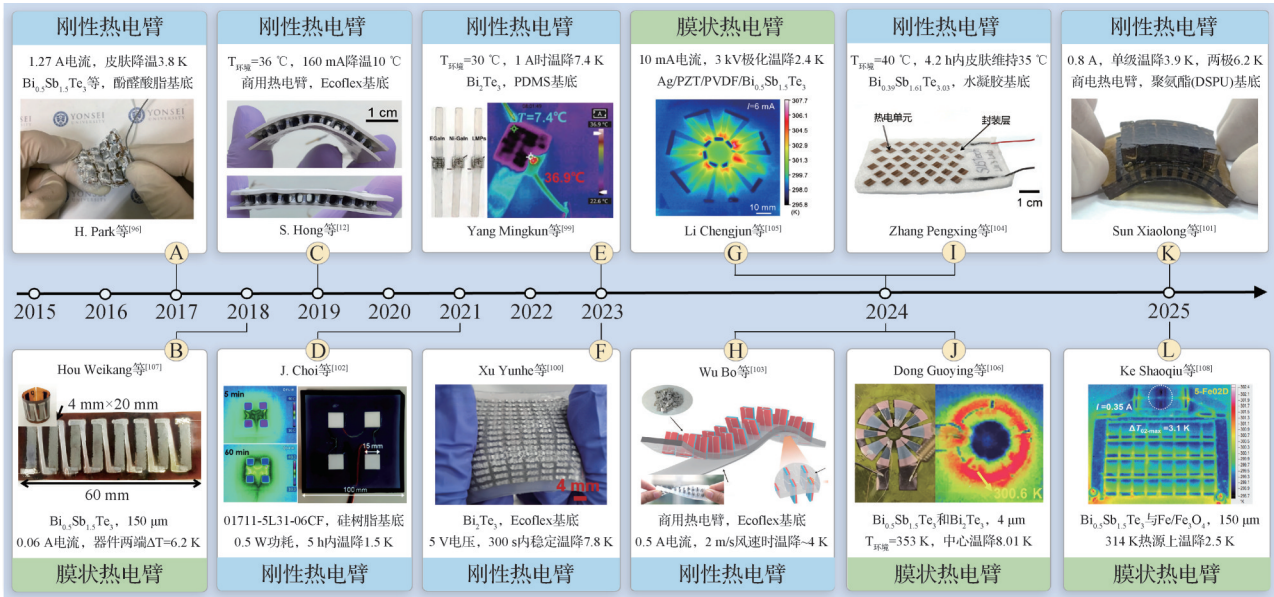


图7 近十年柔性制冷器件的发展历程

Fig.7 The development process of flexible refrigeration devices in the past ten years

### 3 总结与展望

本文综述了近十年柔性热电器件的研究进展,以时间尺度对热电臂制备工艺、器件拓扑方案及其发电、制冷性能进行阐述。定义了热电臂的无量纲特征长度  $L/d$ , 发现  $L/d$  位于大于 10、小于 0.1、介于 0.1~10 时, 分别对应一维纤维器件、二维膜状器件、三维块体器件。一维纤维器件通常采用纤维加捻、拉伸、静电纺丝等方式制成热电纱线, 并集成于织物或其他聚合物基底中, 具备最佳的柔性和穿戴舒适性, 但功率密度较低, 当前归一化功率密度最高为  $0.86 \mu\text{W}/(\text{cm}^2 \cdot \text{K}^2)$ 。二维膜状器件可分为薄膜、厚膜与折叠 3 类: 薄膜器件以磁控溅射等沉积技术为主; 厚膜器件多采用印刷或三维材料减薄技术, 虽然柔性降低但功率密度显著提升至  $30 \mu\text{W}/(\text{cm}^2 \cdot \text{K}^2)$ , 约为薄膜器件的 2 倍; 折叠器件采用卷曲、折叠、多层集成封装等方式, 以柔性换取更高的热电臂密度, 有利于提升功率密度。三维块体器件主要采用商用热电颗粒, 分为填充型与非填充型两类, 柔性相对最差, 但凭借成熟的材料体系, 在皮肤表面已实现  $1.6 \mu\text{W}$  的稳定输出, 具备较好的工程化应用潜力。柔性制冷器件目前还处在初步发展阶段, 当前三维块体器件在皮肤表面最高冷却温差为  $10^\circ\text{C}$ , 二维膜状器件最高制冷温差为  $8^\circ\text{C}$ , 在柔性电子器件冷却方面应用潜力巨大。在结构设计与性能优化方面, 发电与制

冷器件也存在较大差异。柔性发电器件侧重于提升功率密度, 例如缩小膜状热电臂的厚度与间距、构建三维拓扑结构以提升单位面积热电臂数量; 在结构上延长热流传递路径, 从而最大化利用有限温差提升输出电能; 在柔性方面要求较高, 需兼顾可拉伸性及长期动态服役的可靠性。柔性制冷器件更侧重于构建稳定的冷却温差, 例如集成相变材料、水凝胶、翅片结构作为热沉, 处理器件热端产热; 在结构上增加膜状热电臂的厚度, 通过降低电阻以抑制焦耳热, 并采用环形结构使冷量向中心区域集中, 提升热点处理能力; 在柔性方面通常无特殊设计要求。

然而, 柔性热电器件在走向实用化进程中仍面临一些瓶颈: 受限温差与空间下器件输出功率不足、界面热阻引起性能衰减、多次机械形变下的性能退化。针对上述问题, 本文提出 6 个优化方向:

1) 构型革新: 从平面布局到空间拓扑。发展基于折叠、卷曲、多层堆叠的空间拓扑结构, 通过重构热流路径、提升热电臂集成对数, 使有限温差在三维空间中充分利用, 从而在穿戴等受限场景中实现功率密度的提升。

2) 热流定向调控: 从封装缺失到构建梯度热阻。未来封装结构应具备热流引导能力, 通过近热源、冷源侧耦合金属颗粒、碳纳米管等构建高热导界面, 在热电臂周围采用多孔结构、气凝胶等构筑低热导率屏障, 形成“高热导-低热导”梯度结构, 引导热流

定向通过热电臂。

3)可靠性提升:从静态弯曲到动态服役。现有器件通常仅追求最小弯曲半径,难以反映真实穿戴场景下力学状态。未来应完善循环弯曲、拉伸下的性能退化测试、设计应力缓冲结构、选用耐疲劳柔性基材等设计手段,提升器件在长期动态服役下的结构完整性与性能稳定性。

4)贴肤舒适性设计:从刚性接触到仿生设计。在力学上选择PI、PDMS、水凝胶等杨氏模量与皮肤匹配的材料;在界面上应使表面粗糙度达到亚微米量级;在湿热方面建议具备水蒸气透过性,柔性制冷器件需避免瞬时降温超过 $10\text{ }^{\circ}\text{C}$ 引发刺痛感。

5)评价体系完善:从单一冷却温差到综合性能评价。面向未来推广应用,柔性热电制冷器件应构建涵盖最大冷却温差、制冷量、冷却热流密度及COP等参数的综合评价体系;针对穿戴场景,发展精准测试制冷量的方法;同时应推动冷却温差与制冷量测试标准的制定,规范器件发展。

6)系统协同:从分立器件到自供电微系统。单一柔性热电器件输出电压较低,需与最大功率点追踪、低启动电压升压转换电路及微型储能单元一体化集成,构建“采集-转换-存储-供能”闭环的自供电微系统,支撑电子设备的稳定运行。

#### 符号说明

$A$ ——器件面积, $\text{cm}^2$

$L$ ——热电臂的长度, $\text{mm}$

$d$ ——热电臂横截面特征尺寸, $\text{mm}$

$T$ ——温度, $\text{K}$

$\Delta T$ ——器件两端温差, $\text{K}$

$P_{\max}$ ——输出功率, $\mu\text{W}$

$P_{\max}/A$ ——输出功率密度, $\mu\text{W}/\text{cm}^2$

$(P_{\max}/A)/(\Delta T)^2$ ——归一化输出功率密度, $\mu\text{W}/(\text{cm}^2\cdot\text{K}^2)$

#### 参考文献

- [1] Chen Wenyi, Shi Xiaolei, Li Meng, et al. Nanobinders advance screen-printed flexible thermoelectrics[J]. *Science*, 2024, 386(6727): 1265–1271.
- [2] Yuan Xinjie, Qiu Pengfei, Sun Chuanyao, et al. Extraordinary self-powered Y-shaped flexible film thermoelectric device for wearables [J]. *Energy & Environmental Science*, 2024, 17(14): 4968–4976.
- [3] Jiang Yong, Wang Yupeng, Yan Junhao, et al. Research on the performance of thermoelectric self-powered systems for wireless sensor based on industrial waste heat [J]. *Sensors*, 2024, 24(18): 5983.
- [4] Osborn L E, Venkatasubramanian R, Himmtann M, et al. Evoking natural thermal perceptions using a thin-film thermoelectric device with high cooling power density and speed [J]. *Nature Biomedical Engineering*, 2024, 8(8): 1004–1017.
- [5] Yang Qingyu, Yang Shiqi, Qiu Pengfei, et al. Flexible thermoelectrics based on ductile semiconductors [J]. *Science*, 2022, 377(6608): 854–858.
- [6] Gao Yangfan, Zhu Sijing, Gao Jie, et al. Wearable thermoelectric cooler encapsulated with low thermal conductivity filler and honeycomb structure for high cooling effect [J]. *Materials Today Physics*, 2024, 46: 101491.
- [7] Jeong M H, Bae E J, Park B, et al. High-performance and flexible thermoelectric generator based on a robust carbon nanotube/BiSbTe foam[J]. *Carbon Energy*, 2025, 7: e650.
- [8] Lu Yao, Zhou Yi, Wang Wu, et al. Staggered-layer-boosted flexible  $\text{Bi}_2\text{Te}_3$  films with high thermoelectric performance[J]. *Nature Nanotechnology*, 2023, 18(11): 1281–1288.
- [9] Qu Wenmin, Plötner M, Fischer W J. Microfabrication of thermoelectric generators on flexible foil substrates as a power source for autonomous microsystems [J]. *Journal of Micromechanics and Microengineering*, 2001, 11(2): 146–152.
- [10] Cao Tianyi, Shi Xiaolei, Chen Zhigang. Advances in the design and assembly of flexible thermoelectric device [J]. *Progress in Materials Science*, 2023, 131: 101003.
- [11] Yuan Jinfeng, Zhang Yuzhong, Wei Caise, et al. A fully self-powered wearable leg movement sensing system for human health monitoring[J]. *Advanced Science*, 2023, 10(29): 2303114.
- [12] Hong S, Gu Yue, Seo J K, et al. Wearable thermoelectrics for personalized thermoregulation [J]. *Science Advances*, 2019, 5(5): eaaw0536.
- [13] 庞慧梅, 王华才. 碲化锡基热电材料的研究进展[J]. *科学通报*, 2025, 70(6): 645–654. (Pang Huimei, Wang Huacai. Research progress of tin telluride based thermoelectric materials [J]. *Chinese Science Bulletin*, 2025, 70(6): 645–654.)
- [14] 李雨欣, 何文科. 晶界热电材料: 热电参数调控策略及研究进展[J]. *科学通报*, 2025, 70(6): 624–635. (Li Yuxin, He Wenke. Thermoelectric materials with grain boundary: Strategies to parameters [J]. *Chinese Science Bulletin*, 2025, 70(6): 624–635.)
- [15] 宿力中, 冯孝坤. n型硒化锡晶体热电材料研究进展[J]. *科学通报*, 2025, 70(6): 655–664. (Su Lizhong, Feng Xiaokun. Recent progress in n-type SnSe crystals thermoelectric materials [J]. *Chinese Science Bulletin*, 2025, 70(6): 655–664.)

- [16] 邢通, 史迅, 陈立东, 等. 国家自然科学基金视角下我国热能转换技术的研究现状与发展趋势[J]. 科学通报, 2025, 70(32): 5439–5451. (Xing Tong, Shi Xun, Chen Lidong, et al. Status and development trends of the research on thermoelectric technology in China from the perspective of the National Natural Science Foundation of China [J]. Chinese Science Bulletin, 2025, 70 (32) : 5439–5451.)
- [17] Zhang Xiao, Wang Dongyang, Liu Liyao, et al. Irregular hierarchical-porous polymer for high-performance soft thermoelectrics [J]. Science, 2026, 391 (6789) : 1063–1069.
- [18] Zhang Ting, Li Kaiwei, Zhang Jing, et al. High-performance, flexible, and ultralong crystalline thermoelectric fibers[J]. Nano Energy, 2017, 41: 35–42.
- [19] Jang H, Ahn J, Jeong Y, et al. Flexible all-inorganic thermoelectric yarns [J]. Advanced Materials, 2024, 36 (47): 2408320.
- [20] Sun Tingting, Zhou Beiyang, Zheng Qi, et al. Stretchable fabric generates electric power from woven thermoelectric fibers[J]. Nature Communications, 2020, 11: 572.
- [21] Liu Yijie, Wang Xiaodong, Hou Shuaihang, et al. Scalable-produced 3D elastic thermoelectric network for body heat harvesting[J]. Nature Communications, 2023, 14: 3058.
- [22] He Xinyang, Gu Jiatai, Hao Yunna, et al. Continuous manufacture of stretchable and integratable thermoelectric nanofiber yarn for human body energy harvesting and self-powered motion detection [J]. Chemical Engineering Journal, 2022, 450: 137937.
- [23] Lund A, Tian Yuan, Darabi S, et al. A polymer-based textile thermoelectric generator for wearable energy harvesting [J]. Journal of Power Sources, 2020, 480: 228836.
- [24] Lee T, Lee J W, Park K T, et al. Nanostructured inorganic chalcogenide-carbon nanotube yarn having a high thermoelectric power factor at low temperature [J]. ACS Nano, 2021, 15(8): 13118–13128.
- [25] Wu Bo, Wei Wei, Guo Yang, et al. Stretchable thermoelectric generators with enhanced output by infrared reflection for wearable application[J]. Chemical Engineering Journal, 2023, 453: 139749.
- [26] Sun Xiaowen, Yan Yuedong, Kang Man, et al. General strategy for developing thick-film micro-thermoelectric coolers from material fabrication to device integration [J]. Nature Communications, 2024, 15: 3870.
- [27] Yang Dong, Zhang Dongliang, Ao Dongwei, et al. High thermoelectric performance of aluminum-doped cuprous selenide thin films with exceptional flexibility for wearable applications[J]. Nano Energy, 2023, 117: 108930.
- [28] Jin Qun, Zhao Yang, Long Xuehao, et al. Flexible carbon nanotube-epitaxially grown nanocrystals for micro-thermoelectric modules[J]. Advanced Materials, 2023, 35 (46): 2304751.
- [29] Dun Chaochao, Kuang Wenzheng, Kempf N, et al. 3D printing of solution-processable 2D nanoplates and 1D nanorods for flexible thermoelectrics with ultrahigh power factor at low-medium temperatures [J]. Advanced Science, 2019, 6(23): 1901788.
- [30] Hu Qinxue, Liu Weidi, Zhang Li, et al. Carrier separation boosts thermoelectric performance of flexible *n*-type Ag<sub>2</sub>Se-based films [J]. Advanced Energy Materials, 2024, 14 (36): 2401890.
- [31] Wang Dongyang, Ding Jiamin, Ma Yingqiao, et al. Multi-heterojunctioned plastics with high thermoelectric figure of merit[J]. Nature, 2024, 632(8025): 528–535.
- [32] Zhu Wei, Deng Yuan, Cao Lili. Light-concentrated solar generator and sensor based on flexible thin-film thermoelectric device [J]. Nano Energy, 2017, 34: 463–471.
- [33] Wang Xizu, Suwardi A, Lim S L, et al. Transparent flexible thin-film p-n junction thermoelectric module [J]. Npj Flexible Electronics, 2020, 4: 19.
- [34] Wang Yaling, Zhu Wei, Deng Yuan, et al. Self-powered wearable pressure sensing system for continuous healthcare monitoring enabled by flexible thin-film thermoelectric generator[J]. Nano Energy, 2020, 73: 104773.
- [35] Huang Xiaolan, Ao Dongwei, Chen Tianbao, et al. High-performance copper selenide thermoelectric thin films for flexible thermoelectric application [J]. Materials Today Energy, 2021, 21: 100743.
- [36] Lei Yan, Qi Ruijuan, Chen Miaoying, et al. Microstructurally tailored thin  $\beta$ -Ag<sub>2</sub>Se films toward commercial flexible thermoelectrics [J]. Advanced Materials, 2022, 34(7): 2104786.
- [37] Chen Yuexing, Shi Xiaolei, Zhang Junze, et al. Deviceization of high-performance and flexible Ag<sub>2</sub>Se films for electronic skin and servo rotation angle control [J]. Nature Communications, 2024, 15: 8356.
- [38] Tan Ming, Shi Xiaolei, Liu Weidi, et al. Enabling ultra-flexible inorganic thin-film-based thermoelectric devices by introducing nanoscale titanium layers [J]. Nature Communications, 2025, 16: 633.
- [39] Mao Dasha, Zhou Yi, Yu Yong, et al. Scalable and sustainable manufacturing of twin boundary-enhanced flexible Bi<sub>0.4</sub>Sb<sub>1.6</sub>Te<sub>3</sub> films with high thermoelectric performance[J]. Joule, 2024, 8(12): 3313–3323.
- [40] Na J, Kim Y, Park T, et al. Preparation of bismuth

- telluride films with high thermoelectric power factor [J]. *ACS Applied Materials & Interfaces*, 2016, 8 (47) : 32392–32400.
- [41] Karthikeyan V, Surjadi J U, Wong J C K, et al. Wearable and flexible thin film thermoelectric module for multi-scale energy harvesting [J]. *Journal of Power Sources*, 2020, 455: 227983.
- [42] Zhang Jian, Zhang Wenhua, Wei Haoxiang, et al. Flexible micro thermoelectric generators with high power density and light weight [J]. *Nano Energy*, 2023, 105: 108023.
- [43] Toshima N, Oshima K, Anno H, et al. Novel hybrid organic thermoelectric materials: three-component hybrid films consisting of a nanoparticle polymer complex, carbon nanotubes, and vinyl polymer [J]. *Advanced Materials*, 2015, 27(13): 2246–2251.
- [44] Lu Yao, Qiu Yang, Jiang Qinglin, et al. Preparation and characterization of Te/poly(3,4-ethylenedioxythiophene): poly(styrenesulfonate)/Cu<sub>7</sub>Te<sub>4</sub> ternary composite films for flexible thermoelectric power generator [J]. *ACS Applied Materials & Interfaces*, 2018, 10(49): 42310–42319.
- [45] Liu Yan, Zhang Qihao, Huang Aibin, et al. Fully inkjet-printed Ag<sub>2</sub>Se flexible thermoelectric devices for sustainable power generation [J]. *Nature Communications*, 2024, 15: 2141.
- [46] Saeidi-Javash M, Kuang Wenzheng, Dun Chaochao, et al. 3D conformal printing and photonic sintering of high-performance flexible thermoelectric films using 2D nanoplates [J]. *Advanced Functional Materials*, 2019, 29 (35): 1901930.
- [47] Du Jingjie, Zhang Botao, Jiang Meng, et al. Inkjet printing flexible thermoelectric devices using metal chalcogenide nanowires [J]. *Advanced Functional Materials*, 2023, 33(26): 2213564.
- [48] Dai Xu, Wang Yizhuo, Sun Xu, et al. All-automated fabrication of freestanding and scalable photo-thermoelectric devices with high performance [J]. *Advanced Materials*, 2024, 36(21): 2312570.
- [49] Han W B, Heo S Y, Kim D, et al. Zebra-inspired stretchable, biodegradable radiation modulator for all-day sustainable energy harvesters [J]. *Science Advances*, 2023, 9(5): eadf5883.
- [50] Ding Zhaofu, Li Gang, Wang Yejun, et al. Ultrafast response and threshold adjustable intelligent thermoelectric systems for next-generation self-powered remote IoT fire warning [J]. *Nano-Micro Letters*, 2024, 16(1): 242.
- [51] Xiao Zuo, Meng Qiufeng, Du Yong, et al. High-performance Ag<sub>2</sub>Se/methyl cellulose thermoelectric composites for flexible power generators [J]. *Energy Material Advances*, 2024, 5: 103.
- [52] Choi J, Lee J Y, Lee S S, et al. High-performance thermoelectric paper based on double carrier-filtering processes at nanowire heterojunctions [J]. *Advanced Energy Materials*, 2016, 6(9): 1502181.
- [53] Tian Yuan, Florenciano I, Xia Heyi, et al. Facile fabrication of flexible and high-performing thermoelectrics by direct laser printing on plastic foil [J]. *Advanced Materials*, 2024, 36(15): 2307945.
- [54] Hu Mingyuan, Yang Jianmin, Wang Yan, et al. Helical dislocation-driven plasticity and flexible high-performance thermoelectric generator in  $\alpha$ -Mg<sub>3</sub>Bi<sub>2</sub> single crystals [J]. *Nature Communications*, 2025, 16: 128.
- [55] Yin Tingwei, Deng Tingting, Qiu Pengfei, et al. Effects of Ag off-stoichiometry on mechanical and thermoelectric properties of ductile AgCuSe<sub>0.6</sub>Sn<sub>0.4</sub> [J]. *Materials Today Physics*, 2024, 43: 101402.
- [56] Madan D, Wang Zuoqian, Wright P K, et al. Printed flexible thermoelectric generators for use on low levels of waste heat [J]. *Applied Energy*, 2015, 156: 587–592.
- [57] Jung Y S, Jeong D H, Kang S B, et al. Wearable solar thermoelectric generator driven by unprecedentedly high temperature difference [J]. *Nano Energy*, 2017, 40: 663–672.
- [58] Peng J, Witting I, Geisendorfer N, et al. 3D extruded composite thermoelectric threads for flexible energy harvesting [J]. *Nature Communications*, 2019, 10: 5590.
- [59] Kim Y S, Kim H, Yoon T, et al. Latent and controllable doping of stimuli-activated molecular dopants for flexible and printable organic thermoelectric generators [J]. *Chemical Engineering Journal*, 2023, 470: 144129.
- [60] Park S H, Jo S, Kwon B, et al. High-performance shape-engineerable thermoelectric painting [J]. *Nature Communications*, 2016, 7: 13403.
- [61] Varghese T, Dun Chaochao, Kempf N, et al. Flexible thermoelectric devices of ultrahigh power factor by scalable printing and interface engineering [J]. *Advanced Functional Materials*, 2020, 30(5): 1905796.
- [62] Lee D, Park W, Kang Y A, et al. Substrate-free thermoelectric 25  $\mu$ m-thick Ag<sub>2</sub>Se films with high flexibility and in-plane  $zT$  of 0.5 at room temperature [J]. *ACS Applied Materials & Interfaces*, 2023, 15(2): 3047–3053.
- [63] Liu Jinzhuo, Jiang Wangkai, Zhuo Sheng, et al. Large-area radiation-modulated thermoelectric fabrics for high-performance thermal management and electricity generation [J]. *Science Advances*, 2025, 11: eadr2158.
- [64] Wang Liming, Zhang Zimeng, Geng Linxiao, et al. Solution-printable fullerene/TiS<sub>2</sub> organic/inorganic hybrids

- for high-performance flexible n-type thermoelectrics [J]. *Energy & Environmental Science*, 2018, 11(5): 1307–1317.
- [65] Ding Yufei, Qiu Yang, Cai Kefeng, et al. High performance n-type  $\text{Ag}_2\text{Se}$  film on nylon membrane for flexible thermoelectric power generator [J]. *Nature Communications*, 2019, 10: 841.
- [66] Fan Jueshuo, Wang Xiaodong, Liu Fusheng, et al. N-type flexible films and a thermoelectric generator of single-walled carbon nanotube-grafted tin selenide nanocrystal composites [J]. *ACS Applied Materials & Interfaces*, 2021, 13(26): 30731–30738.
- [67] Liu Yuanmeng, Shi Xiaolei, Wu Ting, et al. Boosting thermoelectric performance of single-walled carbon nanotubes-based films through rational triple treatments [J]. *Nature Communications*, 2024, 15: 3426.
- [68] Li Wenhui, Zhang Xuefei, Liu Heng, et al. Two-dimensional van der Waals stack heterostructures for flexible thermoelectrics [J]. *Nano Energy*, 2024, 125: 109605.
- [69] Deng Tingting, Gao Zhiqiang, Qiu Pengfei, et al. High thermoelectric power factors in plastic/ductile bulk  $\text{SnSe}_2$ -based crystals [J]. *Advanced Materials*, 2024, 36(5): 2304219.
- [70] Ding Wenjun, Shen Xinyi, Jin Min, et al. Robust bendable thermoelectric generators enabled by elasticity strengthening [J]. *Nature Communications*, 2024, 15: 9767.
- [71] Wang Yuechu, Li Airan, Hong Youran, et al. Iterative sublattice amorphization facilitates exceptional processability in inorganic semiconductors [J]. *Nature Materials*, 2025, 24: 1545–1553.
- [72] Wang Hong, Li Kuncai, Hao Xin, et al. Capillary compression induced outstanding n-type thermoelectric power factor in CNT films towards intelligent temperature controller [J]. *Nature Communications*, 2024, 15: 5617.
- [73] Ren Wei, Sun Yan, Zhao Dongliang, et al. High-performance wearable thermoelectric generator with self-healing, recycling, and Lego-like reconfiguring capabilities [J]. *Science Advances*, 2021, 7(7): eabe0586.
- [74] Qu Dawei, Li Xin, Wang Hanfu, et al. Assembly strategy and performance evaluation of flexible thermoelectric devices [J]. *Advanced Science*, 2019, 6(15): 1900584.
- [75] Pataki N J, Zahabi N, Li Qifan, et al. A rolled organic thermoelectric generator with high thermocouple density [J]. *Advanced Functional Materials*, 2024, 34(30): 2400982.
- [76] Zhang Dehui, Li Longbin, Zhang Xuanshuo, et al. *In situ* synthesized staggered-layer-boosted flexible  $\text{Ag}_2\text{Se}$  and  $\text{Cu}_2\text{Se}$  thin films for wearable thermoelectric power generators [J]. *Advanced Functional Materials*, 2025, 35(19): 2419392.
- [77] Zhou Qing, Zhu Kang, Li Jun, et al. Leaf-inspired flexible thermoelectric generators with high temperature difference utilization ratio and output power in ambient air [J]. *Advanced Science*, 2021, 8(12): 2004947.
- [78] Zhou Quan, Li Hongxiong, Du Chunyu, et al. High-performance flexible thermoelectric generators with tunable in-plane and out-of-plane architectures [J]. *Nano Energy*, 2023, 118: 109007.
- [79] Zeng Chongyang, Chen Kan, Koz C, et al. Kirigami-inspired organic and inorganic film-based flexible thermoelectric devices with built-in heat sink [J]. *Nano Energy*, 2024, 121: 109213.
- [80] Tao Xudong, Zheng Qianfang, Zeng Chongyang, et al. Cu- or Ag-containing Bi-Sb-Te for in-line roll-to-roll patterned thin-film thermoelectrics [J]. *Nature Communications*, 2025, 16: 196.
- [81] Wu Bo, Guo Yang, Hou Chengyi, et al. From carbon nanotubes to highly adaptive and flexible high-performance thermoelectric generators [J]. *Nano Energy*, 2021, 89: 106487.
- [82] Kim M H, Cho C H, Kim J S, et al. Thermoelectric energy harvesting electronic skin (e-skin) Patch with reconfigurable carbon nanotube clays [J]. *Nano Energy*, 2021, 87: 106156.
- [83] Li Hongxiong, Ding Zhaofu, Zhou Quan, et al. Harness high-temperature thermal energy via elastic thermoelectric aerogels [J]. *Nano-Micro Letters*, 2024, 16(1): 151.
- [84] Wang Yancheng, Shi Yaoguang, Mei Deqing, et al. Wearable thermoelectric generator to harvest body heat for powering a miniaturized accelerometer [J]. *Applied Energy*, 2018, 215: 690–698.
- [85] Kim C S, Yang H M, Lee J, et al. Self-powered wearable electrocardiography using a wearable thermoelectric power generator [J]. *ACS Energy Letters*, 2018, 3(3): 501–507.
- [86] Suarez F, Parekh D P, Ladd C, et al. Flexible thermoelectric generator using bulk legs and liquid metal interconnects for wearable electronics [J]. *Applied Energy*, 2017, 202: 736–745.
- [87] Sugahara T, Ekubaru Y, Van Nong N, et al. Fabrication with semiconductor packaging technologies and characterization of a large-scale flexible thermoelectric module [J]. *Advanced Materials Technologies*, 2019, 4(2): 1800556.
- [88] Zhang Shuai, Liu Zekun, Zhang Wenbin, et al. Multi-bioinspired flexible thermal emitters for all-day radiative cooling and wearable self-powered thermoelectric generation [J]. *Nano Energy*, 2024, 123: 109393.
- [89] Jung Y, Jeong S, Ahn J, et al. High efficiency breathable

- thermoelectric skin using multimode radiative cooling/solar heating assisted large thermal gradient [J]. *Small*, 2024, 20(1): 2304338.
- [90] Jeong M H, Kim K C, Kim J S, et al. Operation of wearable thermoelectric generators using dual sources of heat and light [J]. *Advanced Science*, 2022, 9(12): 2104915.
- [91] Jung S J, Shin J, Lim S S, et al. Porous organic filler for high efficiency of flexible thermoelectric generator [J]. *Nano Energy*, 2021, 81: 105604.
- [92] Han Y, Tetik H, Malakooti M H. 3D soft architectures for stretchable thermoelectric wearables with electrical self-healing and damage tolerance [J]. *Advanced Materials*, 2024, 36(49): 2407073.
- [93] An Zijian, Fu Qiqi, Lü Jingjiang, et al. Body heat powered wirelessly wearable system for real-time physiological and biochemical monitoring [J]. *Advanced Functional Materials*, 2023, 33(34): 2303361.
- [94] Hou Yue, Yang Yang, Wang Ziyu, et al. Whole fabric-assisted thermoelectric devices for wearable electronics [J]. *Advanced Science*, 2022, 9(1): 2270002.
- [95] Jin Junfeng, Hou Yue, Li Chang, et al. High-performance waterproof flexible thermoelectric generators for self-powered electronics [J]. *Nano Energy*, 2024, 132: 110388.
- [96] Park H, Kim D, Eom Y, et al. Mat-like flexible thermoelectric system based on rigid inorganic bulk materials [J]. *Journal of Physics D: Applied Physics*, 2017, 50(49): 494006.
- [97] Cao Lingxiao, Zhang Qiubo, Cen Junfeng, et al. Phase change composite-enabled flexible thermoelectric cooling for personal thermal-regulation [J]. *Journal of Energy Storage*, 2025, 105: 114757.
- [98] Li Peng, Nie Xiaolei, Tian Ye, et al. Fabrication and planar cooling performance of flexible  $\text{Bi}_{0.5}\text{Sb}_{1.5}\text{Te}_3$ /epoxy composite thermoelectric films [J]. *Journal of Inorganic Materials*, 2019, 34(6): 679.
- [99] Yang Mingkun, Li Anqili, Gu Yue, et al. Liquid metal-based flexible and wearable thermoelectric cooling structure and cooling performance optimization [J]. *Science China Materials*, 2023, 66(10): 4001-4011.
- [100] Xu Yunhe, Wu Bo, Guo Yang, et al. Flexible and stretchable thermoelectric devices with Ni-EGaIn liquid metal electrodes for cooling and low-grade-body heat harvesting [J]. *Journal of Alloys and Compounds*, 2023, 945: 169260.
- [101] Sun Xiaolong, Hou Yue, Zhu Zheng, et al. Modular assembly of self-healing flexible thermoelectric devices with integrated cooling and heating capabilities [J]. *Nature Communications*, 2025, 16: 4220.
- [102] Choi J, Dun Chaochao, Forsythe C, et al. Lightweight wearable thermoelectric cooler with rationally designed flexible heatsink consisting of phase-change material/graphite/silicone elastomer [J]. *Journal of Materials Chemistry A*, 2021, 9(28): 15696-15703.
- [103] Wu Bo, Lin Yujie, Tian Yuqing, et al. Bioinspired wearable thermoelectric device constructed with soft-rigid assembly for personal thermal management [J]. *Advanced Functional Materials*, 2024, 34(37): 2402319.
- [104] Zhang Pengxiang, Li Zhiqian, Wang Yupeng, et al. Electronic skin with biomimetic structures realizes excellent isothermal regulation [J]. *Nano Energy*, 2024, 121: 109189.
- [105] Li Chengjun, Li Wang, Sun Chengwei, et al. Enhancing thermoelectric and cooling performance of  $\text{Bi}_{0.5}\text{Sb}_{1.5}\text{Te}_3$  through ferroelectric polarization in flexible Ag/PZT/PVDF/ $\text{Bi}_{0.5}\text{Sb}_{1.5}\text{Te}_3$  film [J]. *ACS Applied Materials & Interfaces*, 2024, 16(34): 45224-45233.
- [106] Dong Guoying, Feng Jianghe, Qiu Guojuan, et al. Oriented  $\text{Bi}_2\text{Te}_3$ -based films enabled high performance planar thermoelectric cooling device for hot spot elimination [J]. *Nature Communications*, 2024, 15: 9695.
- [107] Hou Weikang, Nie Xiaolei, Zhao Wenyu, et al. Fabrication and excellent performances of  $\text{Bi}_{0.5}\text{Sb}_{1.5}\text{Te}_3$ /epoxy flexible thermoelectric cooling devices [J]. *Nano Energy*, 2018, 50: 766-776.
- [108] Ke Shaoqiu, Nie Xiaolei, Wei Ping, et al. Nanomagnetism triggering carriers double-resistance conduction and excellent flexible thermoelectrics [J]. *Advanced Materials*, 2025, 37(10): 2414511.

#### 通信作者简介

申利梅,女,教授,华中科技大学能源与动力工程学院,18674008783, E-mail: ep\_shenlimei@hust.edu.cn,研究方向:热电制冷及发电技术,光电子器件热管理技术。

#### About the corresponding author

Shen Limei, female, professor, School of Energy and Power Engineering, Huazhong University of Science and Technology, 86-18674008783, E-mail: ep\_shenlimei@hust.edu.cn. Research fields: thermoelectric cooling and power generation technology; thermal management in optoelectronic devices.

扫码获取支撑材料



(第二十八届中国科协年会学术论文)